Chin. J. Astron. Astrophys. Vol. 6 (2006), **Suppl. 2**, 97–104
(*http://www.chjaa.org*)

Chinese Journal of
Astronomy and
Astrophysics

Developing Radio Beam Geometry and Luminosity Models of Pulsars

P. L. Gonthier[1] ⋆, S. A. Story[1], B. M. Giacherio[1], R. A. Arevalo[1] and A. K. Harding[2]

[1] Hope College, Department of Physics, 27 Graves Place, Holland, MI 49424, USA
[2] NASA Goddard Space Flight Center, Laboratory for High Energy Astrophysics, Greenbelt, MD 20771, USA

Abstract Our recent studies of pulsar population statistics suggest that improvements of radio and gamma-ray beam geometry and luminosity models require further refinement. The goal of this project is to constrain the viewing geometry for some radio pulsars, especially three-peaked pulse profiles, in order to limit the uncertainty of the magnetic inclination and impact angles. We perform fits of the pulse profile and position angle sweep of radio pulsars for the available frequencies. We assume a single core and conal beams described by Gaussians. We incorporate three different size cones with frequency dependence from the work of Mitra & Deshpande (1999). We obtain separate spectral indices for the core and cone beams and explore the trends of the ratio of core to cone peak fluxes. This ratio is observed to have some dependence with period. However, we cannot establish the suggested functional form of this ratio as indicated by the work of Arzoumanian, Chernoff & Cordes (2002).

Key words: radiation mechanisms:non-thermal — stars: magnetic fields — stars: neutron — pulsars: general

1 INTRODUCTION

A recent population synthesis study (Gonthier et al. 2004) that incorporates the radio beam geometry and luminosity models of Arzoumanian, Chernoff & Cordes (2002) (hereafter ACC) and the geometry and luminosity of the polar cap slot gap model of Muslimov & Harding (2003) simulates the number of radio-loud and radio-quiet (with a radio flux below the survey threshold) γ-ray pulsars detected by the instruments EGRET, AGILE and GLAST. The simulated correlations between the radio and bright γ-ray beam profiles suggest that γ-ray profiles with two peaks have a radio profile that is core dominated with the core peak appearing in between the two γ-ray peaks, which is contrary to the features of most of the EGRET detected γ-ray pulsars that exhibit a single radio peak leading in time the two γ-ray peaks (Thompson 2001). Core-dominated radio emission is implied in the ACC model, especially for young γ-ray pulsars, due to the assumption that the radio core-to-cone peak flux has a $1/P$ period dependence. These findings suggest that a better radio beam model is needed to account for the observed correlations of radio and γ-ray profiles. Motivated by these results, we seek to develop an alternate radio beam geometry and luminosity model by focusing on well defined three-peak radio pulse profiles with adequate polarization data. We fit the polarization position angle within the rotating vector model (RVM) of Radhakrishnan & Cooke (1969) as well as the pulse profiles. While we realize that other possible interpretations of the structure of radio beams are possible, such as the core being a conal structure (Kijak & Gil 2003) or the emitting surface being patchy (Han & Manchester 2001), we assume that pulsars are standard candles, there is a single core beam and a single cone beam characterized by an inner, middle or outer width following Mitra & Deshpande (1999), and the rotating vector model is applicable.

⋆ E-mail: gonthier@hope.edu

2 MODEL

The angular distribution of the core beam is assumed to be a Gaussian centered along the magnetic axis with a characteristic width represented by

$$\begin{aligned} f_{\rm core}(\theta) &= \tfrac{1}{\pi\rho_{\rm core}^2} e^{-\theta^2/\rho_{\rm core}^2}, \\ \rho_{\rm core} &= 1^\circ.5 P^{-1/2}, \end{aligned} \tag{1}$$

where P is the period in seconds and the factor in front of the exponent normalizes the Gaussian. The inclination angle, α, is the angle between the rotational axis and the magnetic axis. The viewing angle, ζ, is the angle between the rotational axis and the viewer. For a given viewing geometry, defined by α and ζ, the polar angle, θ, relative to the magnetic axis is related to the phase angle, ϕ, which is the azimuthal angle relative to the rotational axis, through the expression

$$\cos\theta = \sin\alpha\sin\zeta\cos(\phi - \phi_o^i) + \cos\alpha\cos\zeta, \tag{2}$$

where i = core or cone. The $\phi_o^{\rm core}$ is the phase offset associated with the core beam of the pulsar profile. The characteristic width, $\rho_{\rm core}$, was adopted from ACC model.

The angular distribution of the emitting surface for the conal beam is also parameterized with a Gaussian by the expressions

$$f_{\rm cone}(\theta,\xi) \;=\; \frac{1}{2\pi^{3/2} w_e \bar{\theta}(\beta_{\rm ratio}+1)} \left\{ (\beta_{\rm ratio}-1)\left[1 - \sin\left(\frac{\pi}{2}\sin\xi\right)\right] + 2 \right\} e^{-(\theta-\bar{\theta})^2/w_e^2}, \tag{3}$$

where

$$\begin{aligned} \rho_{\rm cone} &= 4.8^\circ \left(1 + \frac{66}{\nu}\right) P^{-1/2}, \\ \bar{\theta} &= \frac{3}{4}\delta_{\rm r}\rho_{\rm cone}, \text{and} \\ w_e &= \frac{\delta_{\rm w}\rho_{\rm cone}}{4\sqrt{\ln 2}}, \end{aligned}$$

where ξ is the azimuthal angle in the magnetic frame and ν is the observing frequency in MHz. The fitting parameter $\beta_{\rm ratio}$ is introduced to describe an asymmetric conal distribution in order to have the ability to fit conal peaks in the pulse profile that exhibit different maxima. The two fitting parameters, $\delta_{\rm r}$ and $\delta_{\rm w}$, allow for various cones with $\delta_{\rm r}$=0.8, 1.0, and 1.3 for the inner, middle, and outer cones of Mitra & Deshpande (1999). While we do not believe that the conal beam actually has this particular geometry as opposed to say a patchy distribution, this function merely allows us to describe the heights of the two conal peaks in the pulse profile with a function that is easily integrated and, therefore, normalized.

We perform a weighted fit of the position angle, ψ, of the polarization vector with the RVM using the relationship

$$\tan(\psi - \psi_o^{\rm PA}) = \frac{\sin\alpha\sin(\phi - \phi_o^{\rm PA})}{\sin\zeta\cos\alpha - \cos\zeta\sin\alpha\cos(\phi - \phi_o^{\rm PA})}. \tag{4}$$

The phase offset angle, $\phi_o^{\rm PA}$ and the position angle offset, ψ_o, can be obtained for each of the available frequencies, then subtracted from the originals to obtain a global position angle sweep for all frequencies. The inclination angle α and the impact angle β are related to each other by the maximum rate of position angle (PA) sweep $\psi'_{\rm max}$, via,

$$\psi'_{\rm max} = \left(\frac{d\psi}{d\phi}\right)_{\rm max} = \frac{\sin\alpha}{\sin\beta}. \tag{5}$$

Without high quality polarization data, it is not possible to uniquely determine the viewing geometry, α and ζ, from the position angle alone. We fit the global position angle to obtain the maximum rate of change of the position angle,$\psi'_{\rm max}$. While the Stokes parameters I, Q, U and V have standard deviations that obey Gaussian statistics, values derived form these parameters do not. We follow the work of Everett & Weisberg

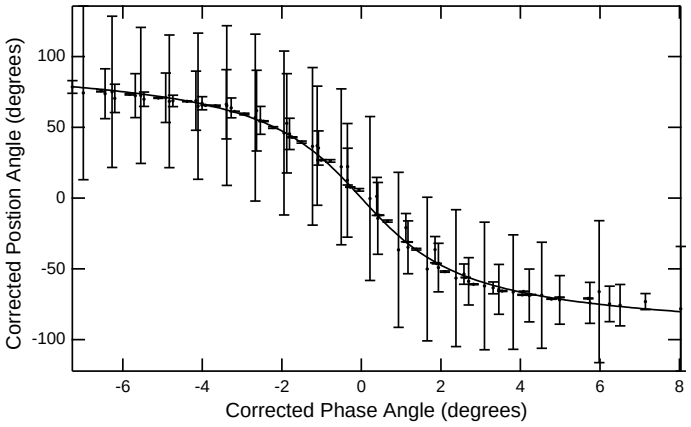

Fig. 1 The global position angle of the pulsar, B2045–16, that combines the data obtained of frequencies of 430, 606, 925, 1408 and 1624 MHz. The smooth curve is the RVM fit.

(2001) in assigning errors to the position angle, ψ. Presented in Figure 1 is the global fit of the PA for pulsar, B2045–16. We have obtained pulse profiles and Stokes parameter profiles from the European Pulsar Network (*http://www.mpifr-bonn.mpg.de/div/pulsar/data/archive.html*).

Assuming the maximum rate of change of the position angle $\psi'_{\rm max}$, we fit the profiles constraining the inclination angle α, and obtain the impact angle, β. Errors in the profile are determined by the standard deviation of the off beam noise. The fitting parameters associated with a component of the profile are the overall amplitude, A_i, and the phase offset, ϕ^i_o, where i=core or cone. The flux in the profile is given by the expression

$$s_i(\theta,\nu) = A_i(\nu) f_i(\theta,\nu), \tag{6}$$

where the f_i term is defined above in Equations (1) and (3). Since the angular distributions are normalized over the emitting surface, the coefficients, A_i, represent the total angle integrated core and cone flux at the particular frequency, ν. However, the width, $\delta_{\rm w}$, and radius, $\delta_{\rm r}$, of the conal annulus are allowed to vary to account for the various cones suggested by the observations. In addition, the parameter, $\beta_{\rm ratio}$ allows for the two peaks of the conal beam in the pulse profile to have different contributions. Assuming a power law with a low frequency cutoff of 50 MHz, the frequency-differential flux has the form

$$s_i(\nu) = -\frac{\alpha_i + 1}{\nu} \left(\frac{\nu}{50\,{\rm MHz}}\right)^{\alpha_i+1} \frac{L_i}{d^2}, \tag{7}$$

where $i =$ core or cone, α_i is the spectral index, d, is the assumed distance to the pulsars and L_i is the angle and frequency integrated luminosity. Having the amplitudes as a function of the available frequencies, a weighted fit can be performed on the spectrum with this function to obtain the luminosity and spectral index of the core and conal components, separately.

Since the maximum rate of change of the PA, $\psi'_{\rm max}$, is the slope of the sweep at the inflection point of the curve, the minimum χ^2_r of the RVM fit to the PA is weakly dependent on the inclination angle, α, as seen in Figure 2(a), where the χ^2_r of the fit is plotted as a function of the maximum rate of change in the PA, $\psi'_{\rm max}$, and α. On the other hand, the χ^2_r obtained from fitting the profile is weakly dependent on the maximum rate of change of the PA, $\psi'_{\rm max}$, as seen in Figure 2(b). Therefore, fitting both the PA and the profile gives a better constraint of the viewing geometry.

The largest uncertainty of the procedure is introduced by the selection of the radius of the annulus parameter, $\delta_{\rm r}$, which defines the inner, middle or outer cone. Values of $\delta_{\rm r} = 0.8, 1.0$ or 1.3 result in different inclination angles. For example in the case of the pulsar, B2045–16, once the maximum rate of change of the PA is established and allowing all parameters to vary while fitting the profile, the minimum $\chi^2_r = 294$ is obtained for $\delta_{\rm r} = 1.00$, $\delta_{\rm w} = 0.65$ and $\alpha = 27.9°$, suggesting the preference for the middle cone. However,

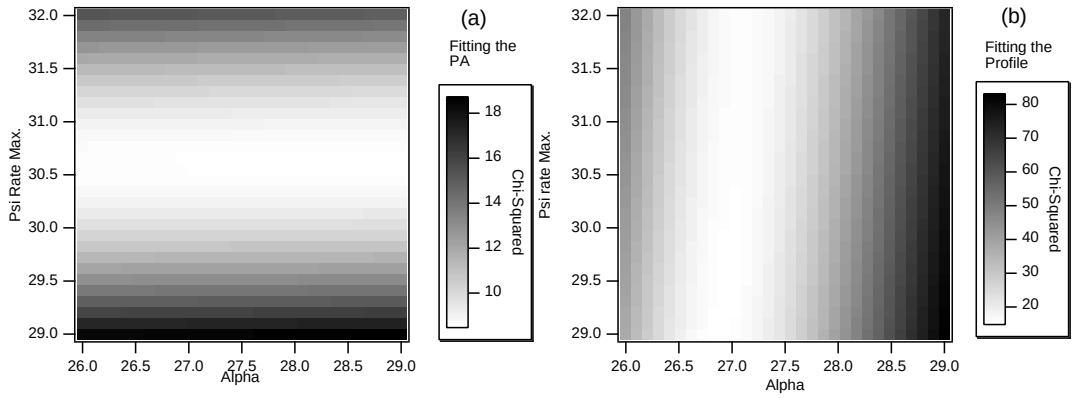

Fig. 2 The reduced χ^2_r obtained from fitting the PA (a) and the profile (b) of the pulsar B2045–16 as a function of the maximum rate of change of the PA, $\psi'_{\rm max}$, and the inclination angle, α, at a frequency of 430 MHz.

as can be seen in Table 1, there is a large variation in the values of α with the conal radius parameter, $\delta_{\rm r}$. Based on the average minimum χ^2_r of 265, the middle cone is selected, and we show in Figure 3 the resulting profiles and fits of the pulsar, B2045–16, for the indicated frequencies.

Table 1 Averages and standard deviations of the parameters and the reduced χ^2_r obtained from fitting the profiles of the pulsar, B2045–16, for the inner, middle and outer cones at the frequencies of 408, 606, 925, 1408 and 1642 MHz.

Cone	$\delta_{\rm r}$	$\delta_{\rm w}$	$\beta_{\rm ratio}$	α	β	χ^2_r
inner	0.8	0.50 ± 0.03	0.76 ± 0.13	$21.7 \pm 0.6^\circ$	$-0.67 \pm 0.02^\circ$	356 ± 410
middle	1.0	0.65 ± 0.04	0.69 ± 0.10	$27.8 \pm 0.7^\circ$	$-0.84 \pm 0.03^\circ$	265 ± 293
outer	1.3	0.93 ± 0.08	0.65 ± 0.09	$37.6 \pm 0.9^\circ$	$-1.10 \pm 0.04^\circ$	544 ± 706

In Figure 4, we plot the core and cone coefficients, $A_{\rm core}$ and $A_{\rm cone}$, representing the angle integrated flux of Equation (6) from the fits of the profiles of pulsar, B2045–16, as a function of the available frequencies indicated. The smooth curves are fits of the power law given in Equation (7), resulting in the indicated total angle and frequency integrated fluxes and spectral indices for the core and cone beams. Using the distances (with ≈20% uncertainty) of the pulsars from the new distance model of Cordes & Lazio (2002), we can estimate the core and cone luminosities.

3 RESULTS

We selected a group of seventeen pulsars ranging in period from 0.06 s (B1913+16) to 3.7 s (B0525+21) whose pulse profiles exhibit a fairly well defined structure consisting of three peaks and have adequate polarization data. We obtained the data from the European Pulsar Database (EPN) with all profiles and polarization data taken in the survey by Gould & Lyne (1998). From the fitting of the position angle sweep and pulse profiles, we obtain the inclination angles, α, the impact angle, β, the spectral indices, fluxes and luminosities of the core and cone beams separately. In Table 2, we compare the extracted inclination α, impact angles β and the maximum rate of change of the PA, $\psi'_{\rm max}$, with the works of Lyne & Manchester (1988) and Rankin (1993). With this information, we are able to estimate the ratio of the core-to-cone peak fluxes, which is independent of the pulsar distance and associated uncertainties. In Figure 5, we present this ratio as a function of the period for three different indicated frequencies. The predictions of the ACC model that assume the ratio of core-to-cone peak flux has a $1/P$ dependence are indicated by dotted lines in each of the panels.

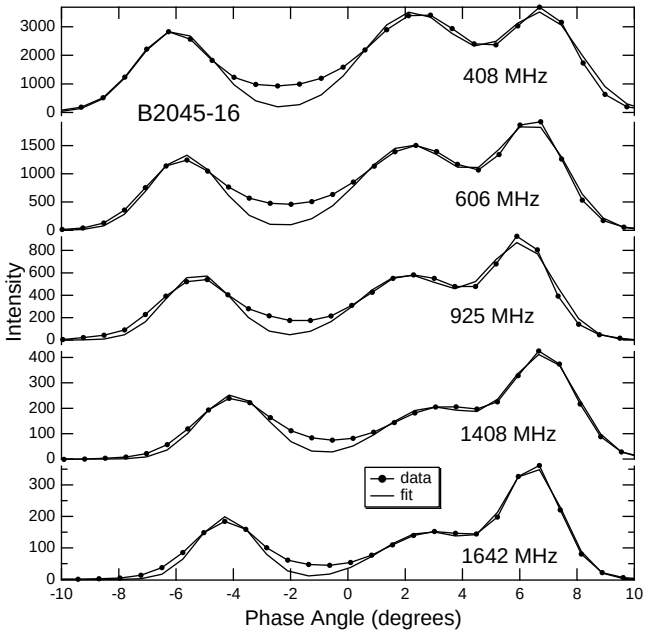

Fig. 3 The pulse profiles (curves with dots) and the fits (smooth curves) of the pulsar B2045–16 at the indicated frequencies.

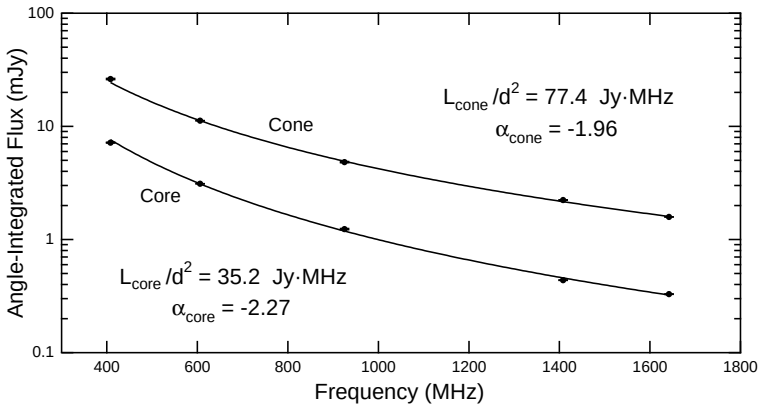

Fig. 4 The core and cone angle integrated fluxes obtained from the fits to the profiles of the pulsar B2045–16 at the frequencies of 408, 606, 925, 1408, and 1642 MHz. Assuming the power law in Equation (7), the fluxes are fit to obtain the indicated angle and frequency integrated fluxes and spectral indices.

The period dependence of the ratios indicates a break around a period of 0.7 seconds. We parameterize the period and frequency dependence of the ratios below and above 0.7 s. We find that the ratio of the core-to-cone increases as $P^{1.5}\nu^{-1}$ up to 0.7 seconds and then decreases as $P^{-3}\nu^{-1}$. The results are quite different than those of the ACC model, particularly for the behavior of the ratio core-to-cone peak flux for short period pulsars. Our results suggest that they are not as core-dominated as implied by an extrapolation of the ACC model.

Table 2 Inclination angles α, impact angles β, and maximum rate of change of PA $\psi'_{\rm max}$ obtained from fits are compared to the studies of Lyne & Manchester (1988) and Rankin (1993). In the fits $\alpha \leq 90^\circ$ and β and $\psi'_{\rm max}$ have the same signs.

Pulsar		This Work			Lyne & Manchester			Rankin		
Name	Period (s)	α	β	$\psi'_{\rm max}$	α	β	$\psi'_{\rm max}$	α	β	$\psi'_{\rm max}$
B1913+16	0.0590	44	–0.8	–52				46	–0.8	–51
B1804–08	0.1637	51	3.5	13	47	2	21	63	5.1	10
B1702–19	0.2990	45	5.7	7	90	4.1	14	85	4.1	14
B2048–72	0.3413	35	–2.3	–14	29	–1.4	–20			
B1839+09	0.3813	90	2.6	22	90	2.9	20	83	1.4	42
B0727–18	0.5102	25	–4	–7	28	–6.8	–4			
B2003–08	0.5809	19	–3.7	–5	13	–3.1	–4	13	–3.3	–4
B1845–01	0.6594	42	–3.2	–12						
B1508+55	0.7397	35	2.9	11	80	2	28	45	2.7	15
B1821+05	0.7529	27	2.9	10	28	1.5	18	32	1.7	18
B2111+46	1.0147	10	1.1	9.1	8.6	1.3	6.7	9	1.4	6.7
B1039–19	1.3864	24	1.3	18	34	1.8	18	31	1.7	18
B2045–16	1.9616	27	0.8	31	37	1.1	30	36	1.1	30
B0525+21	3.7455	14	–0.4	–35	23	–0.7	–31	21	–0.6	–36

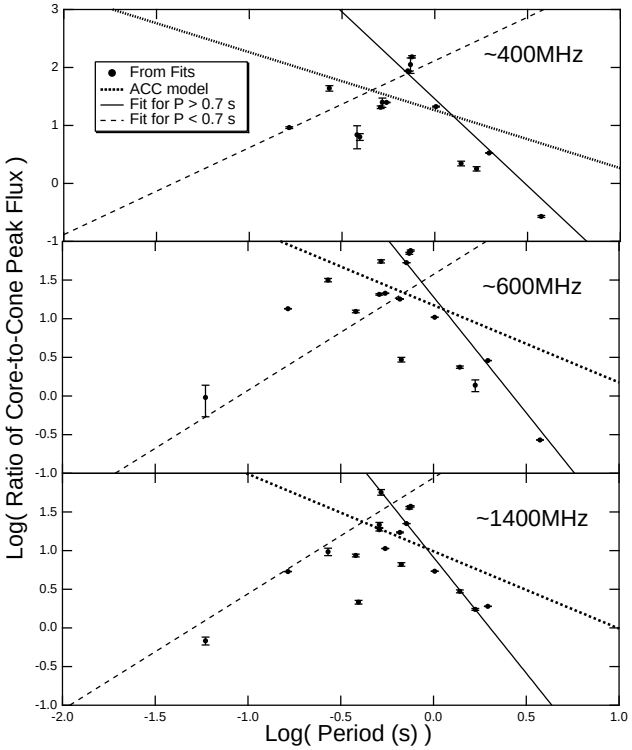

Fig. 5 The logarithm of the ratio of the core-to-cone peak flux is plotted as a function of the logarithm of the pulsar period for the indicated frequencies. The predictions of the ACC model are indicated by dotted lines. The dashed and solid lines represents the parameterization of the ratios below and above 0.7 seconds, respectively (see text).

With the extracted fit parameters, we are able to estimate the luminosity of the core and cone beams separately, as shown in Figure 6. The bottom part of the figures displays the luminosity of the cone beam (solid dots) with a parameterized function suggested by the fits (crossed circles). The functional dependence of period and period derivative is indicated in the figure for the parameterization. Likewise the luminosity of the core is displayed in the middle portion of the figure. The total luminosity is shown at the top of the figure along with the predictions of the ACC model.

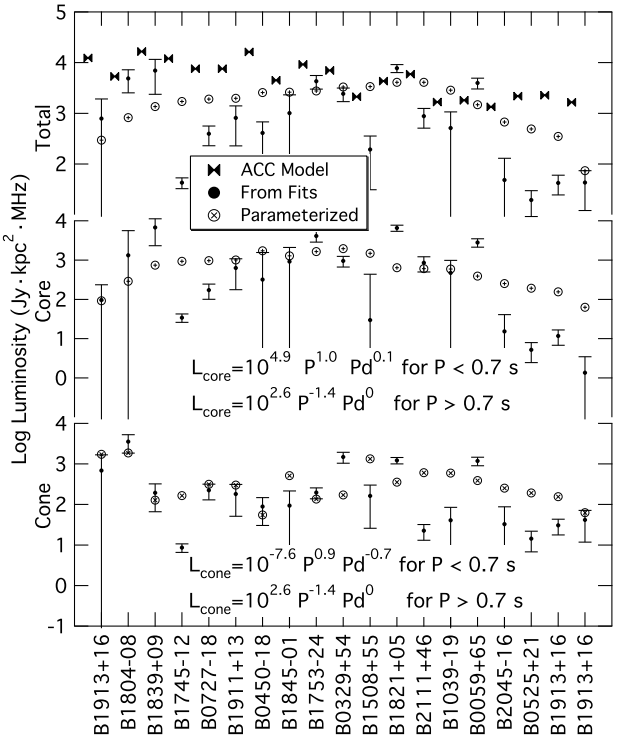

Fig. 6 The logarithm of the total (top), core (middle) and cone (bottom) luminosities obtained from the fits (solid dots), parameterization (circles with crosses) and predictions of ACC model (top).

4 CONCLUSIONS

We focus on a select group of pulsars that exhibit three peaks in their pulse profiles with adequate polarization data. We find that there are a very limited number of these pulsars on the EPN database with good polarization data. All of polarization data in this study comes from the survey of Gould & Lyne (1998). We fit both the position angle as well as the pulse profile intensities with a simple model that assumes a single core beam and a single cone beam. Assuming a standard period dependence of the characteristic widths (Equations (1) and (3)) and the presence of three conal beams as described by Mitra & Deshpande (1999), we find that the ratio of the core-to-cone peak flux for short period pulsars does not follow the $1/P$ trend suggested by the study of Arzoumanian, Chernoff & Cordes (2002). There appears to be a break in the period dependence of the ratio near a period of 0.7 seconds, with the ratio decreasing for short period pulsars. Such a result alters significantly the interpretation of radio profiles of short period pulsars and requires further study.

The interpretation of radio profiles in young high-energy pulsars is not well established. While Arzoumanian, Chernoff & Cordes (2002) proposed both a beam geometry and a luminosity model of the

core and cone radio beams, a considerable controversy exists in the interpretation of single peaked radio pulse profiles, as to whether the origin is from core emission or partial cones (Manchester 1996). The study presented in this paper and others like it may help in understanding the geometry of radio emission from pulsars, particularly from young pulsars. Our study indicates that the ACC model requires some revision in regards to the ratio of the core-to-cone emission for short period pulsars.

Acknowledgements We express our gratitude for the generous support of the Michigan Space Grant Consortium, of Research Corporation (CC5813), of the National Science Foundation (REU and AST-0307365) and the NASA Astrophysics Theory Program.

References

Arzoumanian, Z., Chernoff, D.F., & Cordes, J.M., 2002, ApJ, 568
Cordes, J.M., Lazio, T.J.W., 2002, Astro-ph/0207156
Everett, J.E., Weisberg, J.M., 2001, ApJ, 553, 341
Gonthier, P.L., Van Guilder, R., Harding, A.K., 2004, ApJ, 604, 775
Gould, D.M., Lyne, A.G., 1998, MNRAS, 235
Han, J. L., Manchester. R.N., 2001, MNRAS, 320, L35
Kijak, J., Gil, J., 2002, A&A, 392, 189
Lyne, A. G., Manchester, R.N., 1988, MNRAS, 234, 477
Manchester, R. N., 1996, in ASP Conf. Ser. 105, Pulsars: Problems and Progress, 160th Colloq. IAU, ed. S. Johnson, M. A. Walker, M. Bailes (San Francisco: ASP), 193
Mitra, D., Deshpande, A.A., 1999, A&A, 346, 906
Muslimov, A. G. Harding, A. K., 2003, ApJ, 588, 430
Radhakrishnan, V., Cooke, D.J., 1969, ApJ, 3, 225
Rankin, J. M., 1993, Ap&SS, 85, 145
Thompson, D. J., 2001, In: F. A. Aharonian and H. J. Völk. eds., AIP Conf. Proc. 558, High Energy γ-Ray Astronomy, New York: AIP, 103